

Continuous Monitoring with a Superconducting Gravimeter As a Proxy for Water Storage Changes in a Mountain Catchment

Quentin Chaffaut, Jacques Hinderer, Frédéric Masson, Daniel Viville, Jean-Daniel Bernard, Solenn Cotel, Marie-Claire Pierret, Nolwenn Lesparre, and Benjamin Jeannot

Abstract

In mountainous area, spring water constitutes the only drinking water resource and local economy is highly dependent on forest health and productivity. However, climate change is expected to make extreme water shortage episodes more and more frequent. Forest is therefore more and more exposed to water stress. It appears necessary to quantify the drought induced by water deficit to evaluate forest vulnerability and to plan the future of forest management. In this study we quantified the 2018 water deficit experienced by the forest in the Strengbach catchment, located in the French Vosges mountains. Three methods for estimating catchment water storage changes (WSC) have been compared. The first relies on superconducting gravimeter monitoring while the second relies on catchment water balance. The third one relies on global hydrological model MERRA2. We show that WSC estimated from measured gravity changes correlate well with WSC estimated from catchment water balance while WSC inferred from MERRA2 significantly differs. The Strengbach catchment water cycle is mostly annual but exhibits significant interannual variability associated with the 2018 drought episode: August 2018 has a water deficit of 37 mm (as inferred from catchment water balance) or 76 mm (as seen with superconducting gravimetry) compared to August 2017. We illustrate here the use of superconducting gravimeter monitoring as an independent proxy for WSC in a mountainous catchment while most of hydro-gravimetric studies have been conducted on relatively flat areas. We therefore contribute to expand the area of use of high precision gravity monitoring for the hydrological characterization of the critical zone in mountainous context. This innovative method may help to assess forest vulnerability to drought in the context of climate change.

Keywords

Hydro-gravimetry · Hydrological modeling · Mountain catchment · Superconducting gravimetry

Q. Chaffaut (✉) · J. Hinderer · F. Masson · J.-D. Bernard
IPGS-EOST, CNRS-UMR 7516, University of Strasbourg, Strasbourg,
France
e-mail: qchaffaut@unistra.fr

D. Viville · S. Cotel · M.-C. Pierret · N. Lesparre
LHyGeS-EOST, CNRS-UMR 7517, University of Strasbourg,
Strasbourg, France

B. Jeannot
LHyGeS-ENGES, CNRS-UMR 7517, University of Strasbourg,
Strasbourg, France

1 Introduction

Spring water constitutes the only drinking water resource for villages located in the French Vosges mountains. Furthermore, local economy (tourism, hunt, logging, wood transformation) is highly dependent on forest health and productivity. However, the forest welfare is highly sensitive to water shortage associated with severe drought e.g. the 2003 western European drought episode or the 2012–2015 California drought (Bréda et al. 2006; Asner et al. 2016). Unfortu-

nately, climate change is expected to increase temperature variability and to enhance the frequency and the severity of such drought events, especially in the northern hemisphere (Seneviratne et al. 2012). This may compromise long-term tree survival in some part of the Vosges mountains, especially because of combined effect of water stress, decrease of fertility and parasite attack. It is thus necessary to assess water storage changes (WSC) at the catchment scale to compute a posteriori water deficit experienced by the forest.

Catchment WSC result from the water fluxes acting in the landscape, balancing precipitation, evapotranspiration and runoff. Classically, there are two ways for estimating WSC at the catchment scale in mountainous areas: one may rely on local prediction from global hydrological models or on catchment water balance derived from local hydro-meteorological measurements. On the first hand, global hydrological models provide soil WSC but with a sparse spatial resolution. On the other hand, catchment water balance is representative of catchment WSC but is still particularly difficult to assess from local hydro-meteorological measurements in a mountainous context because topography or land-cover variations make rainfall and evapotranspiration fluxes highly heterogeneous and consequently difficult to monitor (Shamir et al. 2016).

A third option to estimate WSC is the use of in situ time-variable gravimetry that is a non-invasive method, in contrast to traditional point scale measurements used for directly measuring soil WSC e.g. with neutron probes (Hector et al. 2013). Time-variable gravimetry is also directly sensitive to integrated WSC and so bridges the gap between point scale measurements and large-scale estimates of WSC (Fores et al. 2017). It therefore appears as a well-suited method to assess WSC at the catchment scale independently from hydro-meteorological measurements.

With a nominal precision of 0.1 nm.s^{-2} , the superconducting gravimeter (SG) is the most sensitive relative gravimeter available (see Hinderer et al. 2015 for a review). The SG gravity signal contains several geophysical, atmospheric and hydrological contributions listed hereafter. The strongest contribution is the tidal signal from oceans and solid Earth due to the attraction of Moon and Sun. The tidal signal produces gravity variations up to $2,800 \text{ nm.s}^{-2}$. The polar motion is another signal of external origin resulting from the motion of the Earth rotational axis, it produces gravity variations up to 100 nm.s^{-2} . Hydrological and atmospheric signals seen by the SG strongly depend on climatic conditions and on the local geomorphological context. Both hydrological and atmospheric signal contains a local contribution as well as a non-local contribution resulting from large-scale atmosphere and hydrology. Large-scale contributions are estimated thanks to global atmospheric and hydrological models (Llubes et al. 2004; Boy et al. 2002). The total (local + non-local) hydrological contribution produces grav-

ity variations usually up to 150 nm.s^{-2} and the total atmospheric contribution produces gravity variations of the same order of magnitude. Nowadays, the hydro-gravimetric signal i.e. the gravity signal corrected for every other well modelled instrumental and geophysical contributions becomes relatively easy to extract. As a result, hydro-gravimetric studies using SG dedicated to local WSC monitoring become more and more common (e.g. Hector et al. 2014; Fores et al. 2017).

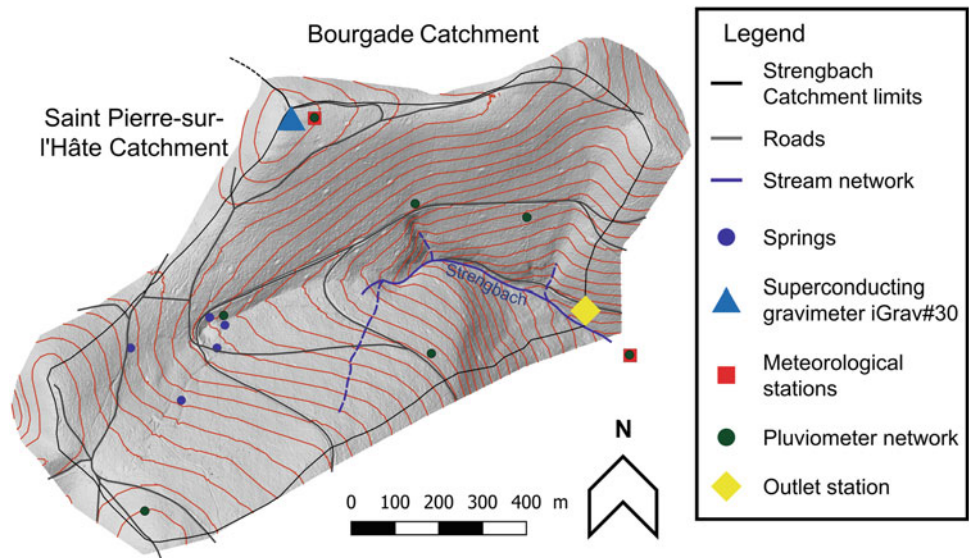
However, most of hydro-gravimetric studies relying on SG focus on the hydrology of relatively flat areas like plains or plateaus. Here we apply in situ superconducting gravity monitoring to the hydrological characterization of a mountainous catchment. Here hydrological contributions are due to fast changes in soil water storage associated with precipitations (hourly timescale or less) or slower changes associated with underground flow which produces gravity variations up to 150 nm.s^{-2} . Due to its strong topography, our study site exhibits a very reactive hydrological behavior as well as an a priori complex spatial distribution of water. This last point certainly constitutes our main challenge because gravity does not depend only on the water amount but on the spatial distribution of water too.

Here we assume that SG hydrological residual signal acts as a daily proxy of WSC at the catchment scale in a forested mountainous area and brings new independent constraints to test catchment WSC derived from catchment water balance on one hand or predictions of global hydrological model MERRA2 (Reichle et al. 2017) on the other hand.

2 Study Site: The Strengbach Catchment

The Strengbach catchment is a small (0.8 km^2) forested catchment located on the western side of the Vosges mountains in France (Fig. 1). It corresponds to the site of OHGE i.e. Hydro-Geochemical Observatory of the Environment (<http://ohge.unistra.fr>) which is part of the OZCAR network for the study of the critical zone (<http://ozcar-ri.prod.lamp.cnrs.fr>). A part of water from four springs located on the site is taken as drinking water for the village. The Strengbach catchment is a granitic catchment with altitudes ranging between 883 m at the outlet and 1,146 m at the summit. The bedrock mainly consists in Brezouard granite and is covered by a granitic saprolite whose thickness varies between 1 and 9 m (Pierret et al. 2018). This thin superficial layer is expected to host the active aquifer i.e. the main contributor of the stream draining of the Strengbach catchment (Weill et al. 2017). Catchment runoff is measured at the outlet station while meteorological measurements are provided by the summit weather station and by a network of pluviometers distributed across the catchment (Fig. 1). Evapotran-

Fig. 1 Strengbach catchment topography and localization of hydro-meteorological and superconducting gravity measurements. Vertical distance between iso-level lines is 10 m



spiration is modeled from meteorological measurements. In this way, OHGE observatory provides the catchment water balance computed from the modeled and monitored hydro-meteorological fluxes.

In the framework of the CRITEX project (<https://www.critex.fr>) a new superconducting gravimeter iGrav#30 (SG) from GWR Instruments Inc. has been installed in June 2017 at the summit of the Strengbach catchment in the vicinity from the meteorological station (Fig. 1). SG is installed on the edge of a $8.4 \text{ m} \times 4.4 \text{ m}$ shelter with concrete foundations but no gravimetric pillar. In this way WSC occur only at a smaller altitude than the SG and every area located in the footprint of the gravimeter contribute positively to the gravity signal measured by the SG i.e. a water storage increase induces a gravity increase. This specific location maximizes the hydro-gravimetric signal and enable the use of SG hydro-gravimetric signal as a proxy of local WSC. Note that the SG shelter acts as a mask which prevent water to infiltrate beneath the gravimeter (Creutzfeldt et al. 2010; Deville et al. 2013; Reich et al. 2019). The resulting mask effect is quantified in a next section.

3 Data and Methodology

3.1 Extraction of Hydro-Gravimetric Signal from Superconducting Gravimeter Data

The raw output of SG is a voltage that needs to be converted into gravity units by means of calibration. The calibration process consists in adjusting the scale factor of the SG with side by side observations during several days using an absolute gravimeter FG5#206 from Micro-g Lacoste Inc. (Rosat et al. 2018). At least one other absolute measurement

is necessary to constrain the long-term instrumental drift. The calibration factor of SG is $-919 \pm 3 \text{ nm.s}^{-2}.\text{V}^{-1}$ and the instrumental drift is $70 \text{ nm.s}^{-2}.\text{year}^{-1}$. Since we only have two absolute gravity measurements at our disposal, we couldn't assess the linearity of the long-term drift. However, this last one is well approximated by linear polynomial in a long-term view as indeed observed on other SGs (Fores et al. 2017; Rosat et al. 2018).

Being part of the IGETS network (previously GGP see Crossley and Hinderer 2010), level 1 SG raw data are available at <https://isdc.gfz-potsdam.de/igets-data-base/>. First pre-processing step consists in decimating second samples into minute samples using a standard low pass filter. Then spikes resulting from visits in the SG shelter or earthquakes are removed. After this preprocessing step, data are corrected for the long-term instrumental drift and for polar motion the last one being provided by the International Earth Rotation Service (<ftp://hpiers.obspm.fr/iers/eop/eopc04/>).

We separate tidal, hydrological and atmospheric contributions that are present in the SG gravity signal by introducing a priori atmospheric and hydrological corrections prior to the tidal model adjustment. We compute the input data of tidal analysis by correcting iGrav#30 gravity from instrumental drift, polar motion, theoretical annual and semi-annual tides (delta factor 1.16 and lag 0°), atmospheric and hydrological loading. Then shorter period tides (monthly to half-daily tides) are adjusted by the tidal analysis version ET34-X-V71 of ETERNA (Schueller 2015). Both atmospheric and hydrological loading processes are decomposed into a local newtonian component (distance $< 11 \text{ km}$ from the gravimeter) and a non-local newtonian+elastic component which account for large-scale (non-local) atmosphere and hydrology contributions. Non-local atmospheric loading is

computed by convolving Green's function with a 2.5D atmospheric density model based on ECMWF surface pressure fields (Boy et al. 2002). Local atmosphere (distance up to 11 km from the gravimeter and 30 km above the topography) is discretized into prisms. The air density profile is derived from local surface pressure measurement using the perfect gas law and assuming hydrostatic equilibrium at each time-step. Local atmospheric loading is then computed by summing up the gravity effect of all prisms using the integration method described in (Leirião et al. 2009). Non-local hydrological loading is computed by convolving Green's functions with non-local MERRA2 cell elements (Llubes et al. 2004; Reichle et al. 2017). MERRA2 is a global hydrology model based on a land surface model forced by atmospheric parameters such as precipitation, temperature and solar radiations. Local hydrological loading is computed by converting the catchment water balance into a gravity signal assuming a homogeneous water coverage over the topography (see next section for a detailed explanation). The last processing step for extracting the local hydrological contribution (the so-called hydrological residual) from the SG signal consists in correcting the tidal analysis input data by removing the adjusted tidal model and adding back the modeled local hydrological loading (removed prior to the tidal analysis).

3.2 Converting the Local Hydro-Gravimetric Signal into Water Storage Changes at the Catchment Scale

The Strengbach catchment is defined topographically so that the watershed limit corresponds to the crest line. In such hydrological catchment, borders act as no-flow conditions and runoff is collected fully at the outlet. Therefore, catchment water storage depends only on input flux i.e. rainfall and output flux i.e. runoff and evapotranspiration. Runoff is measured at the outlet of the catchment, mean annual runoff is 697 mm for the period 2014–2018. Evapotranspiration is modeled using the BILJOU model (Granier et al. 1999) by considering the forest cover and soil type and using solar radiation, temperature, humidity and wind speed measurements from the summit weather station; its mean annual value is 418 mm for the same 2014–2018 period. Rainfall is measured every 10 min by an automatic rain gauge located at the summit weather station. In parallel, repeated measurements (2-week sampling rate) of a network of rain gauges distributed across the catchment allow to measure spatial heterogeneity of rainfall. The combination of both datasets allows to upscale the catchment mean hydrological rainfall (the rainfall amount that effectively reaches the surface) from the automatic rain gauge measurement. The mean

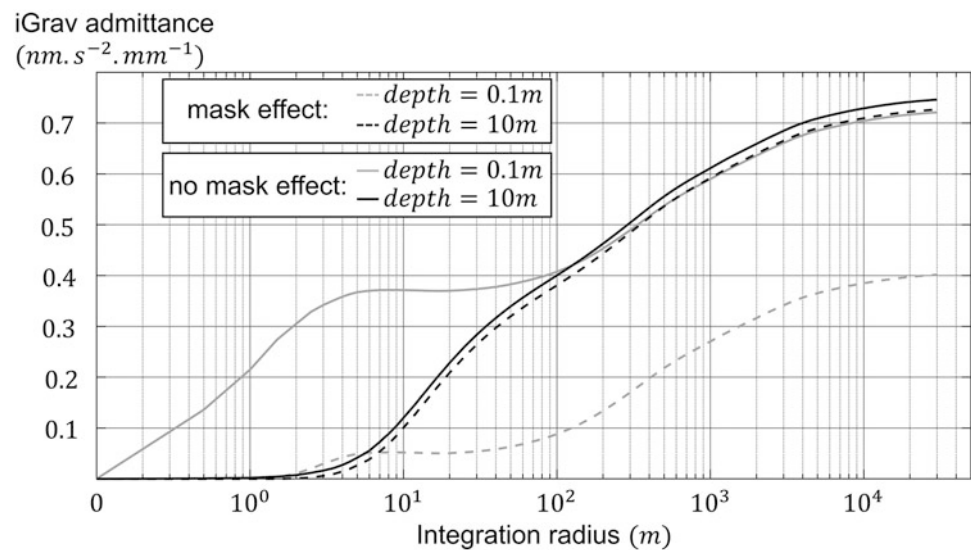
annual hydrological rainfall is 1,194 mm including 20% of snow for the 2014–2018 period. Based on measured input and output water fluxes, we compute the catchment WSC at a daily time step according to the water-balance equation:

$$\begin{aligned} \text{WaterStorageChanges}(t) &= \text{Rain}_{\text{cumulated}}(t) - \text{Runoff}_{\text{cumulated}}(t) \\ &\quad - \text{EvapoTranspiration}_{\text{cumulated}}(t) \end{aligned} \quad (1)$$

For comparison with catchment water balance and MERRA2 local, we need to convert SG hydro-gravimetric signal expressed in nm.s^{-2} into WSC expressed in mm of water. The measured gravity response associated with catchment WSC depends on the amount of WSC as well as on the location of WSC. The hydro-gravimetric signal is also impacted by the mask effect: the SG shelter acts as an impermeable layer which reduce WSC in the close surrounding of the gravimeter (Creutzfeldt et al. 2010; Deville et al. 2013; Reich et al. 2019). Here we assume that the ground WSC occurs mainly in the thin granitic saprolite soil layer which hosts the active aquifer of the Strengbach catchment (Weill et al. 2017). Based on this consideration, we model catchment WSC as a spatially homogeneous water layer of time-variable thickness placed at a given depth below the ground surface. A water layer of nominal thickness (0.1 m) is discretized into prisms whose horizontal extension is $0.5 \text{ m} \times 0.5 \text{ m}$. Then we compute the water admittance at the SG location i.e. the gravity response of a water layer of nominal thickness evaluated at SG location (Fig. 2). We do this by summing up the gravity effects of prisms using the integration method described in (Leirião et al. 2009): for a normalized distance (i.e. the ratio between prism size and prism distance from SG) below 25 [–] we use the prism formula, for a normalized distance between 25 and 36 [–] we use the Macmillan formula (an approximation of the prism formula) and for a normalized distance bigger than 36 [–] we use the point-mass formula.

As a first step, we compute the unmasked water admittance i.e. we neglect the mask effect by summing up the gravity effect of all prisms for integration radius ranging from 0 to 30 km away from SG. We compute it for a water layer depth of 0.1 m or 10 m (Fig. 2). It converges to (respectively) $0.71 \text{ nm.s}^{-2}.\text{mm Water}^{-1}$ or $0.73 \text{ nm.s}^{-2}.\text{mm Water}^{-1}$, it means that the unmasked admittance asymptotic value is almost not sensitive to the depth of the water layer. However, it should be noted that the vertical distribution of water has a significant effect on the unmasked admittance up to 100 m of distance from the SG (note the difference between solid lines for an integration radius ranging from 0 to 100 m on Fig. 2). In a next step we compute the masked admittance by excluding the prisms from below the shelter:

Fig. 2 Solid lines: unmasked admittance for a water layer depth of 0.1 m (light grey) or 10 m (dark grey). Dotted lines: masked admittance for a water layer depth of 0.1 m (light grey) or 10 m (dark grey)



i.e. we assume there is no WSC occurring below the shelter. For a depth of 0.1 m masked admittance reaches only $0.43 \text{ nm.s}^{-2}.\text{mm Water}^{-1}$ while it converges to $0.71 \text{ nm.s}^{-2}.\text{mm Water}^{-1}$ for a depth of 10 m, which almost correspond to the unmasked admittance value. Therefore, the magnitude of the mask effect and then the masked admittance asymptotic value depends heavily on the vertical distribution of water: the more the water layer is shallow, the more the mask effect is significant. In the absence of any other observational constraints on the vertical distribution of water around the SG, it results that masked admittance ranges between 0.43 and $0.71 \text{ nm.s}^{-2}.\text{mm Water}^{-1}$.

Both masked and unmasked admittance reach 90% of their asymptotic value for an integration radius of 5 km, which gives an estimate of the SG footprint (Fig. 2) It means that most of the local hydrological signal comes from a circle of 5 km radius centered at SG location. SG is therefore sensitive to WSC occurring in the three contiguous catchments (see Fig. 1).

4 Results and Discussion

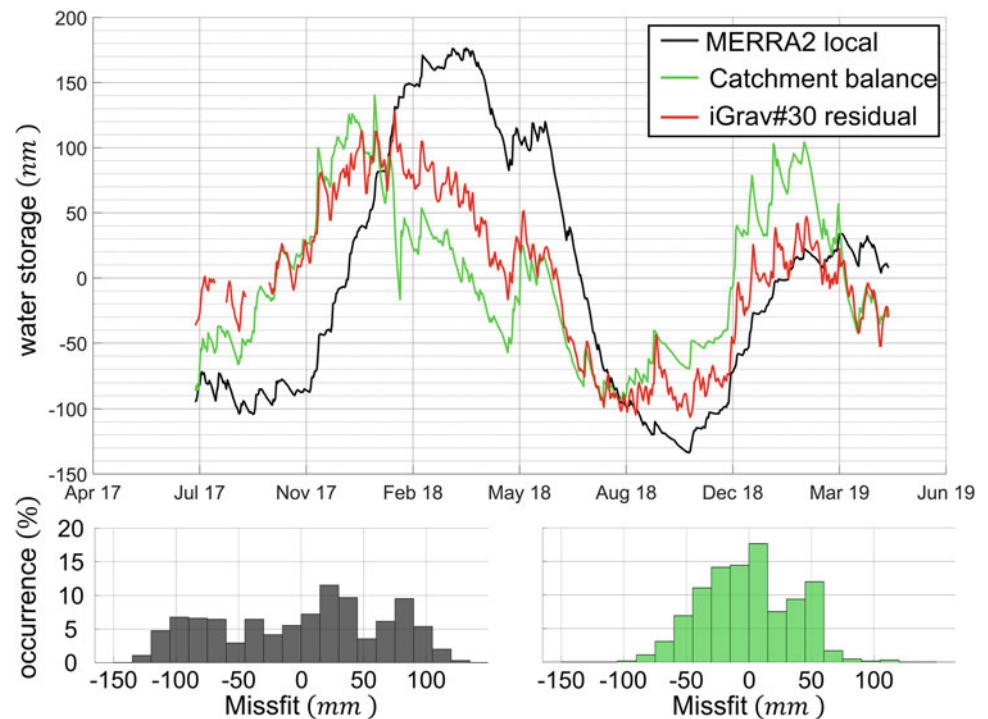
SG hydro-gravimetric signal and catchment water balance are compared in terms of WSC expressed in mm of water (Fig. 3). The admittance value used to convert SG gravimetric signal (in nm.s^{-2}) into WSC (in mm of water) is adjusted by scaling the SG signal on the catchment water balance. The adjusted admittance we found is $0.60 \pm 0.02 \text{ nm.s}^{-2}.\text{mm Water}^{-1}$ which lies within the range of computed masked admittance values (Fig. 2).

The root mean square difference between zero-averaged SG and catchment balance WSC is 36 mm of water. Gravity and hydro-meteorological estimates of WSC are conse-

quently in good agreement which is remarkable considering the numerous corrections applied on gravity data as well as the simplistic hypothesis we made to convert water storage into gravity. Note that a part of the remaining discrepancy between gravity WSC and catchment WSC may be due to a residual instrumental drift in the SG signal. Instrumental drift will be better constrained thanks to new absolute measurements planned in the future. SG is located at the junction point between three different catchments: The Strengbach catchment on the South East, the Bourgade catchment on the North East and the Saint Pierre Sur L'Hôte catchment on the South West (Fig. 1). It is therefore sensitive to WSC occurring in these three catchments. As we succeed to reproduce the measured hydro-gravimetric signal by extrapolating the Strengbach catchment WSC within the footprint area of the gravimeter, it suggests that: (1). SG hydro-gravimetric signal may be considered as a new independent proxy of water storage in the Strengbach catchment. (2) Despite their different orientations, geology, forest cover, etc. these three catchments may have a similar hydrological behavior.

Both SG and catchment water balance exhibit fast (daily to weekly) WSC but the water cycle is dominated by a seasonal component with significant interannual variability. Minimum and maximum water storage occurs merely at the same time every year. For both 2017 and 2018 the minimum water storage occurs at the end of August and the maximum water storage occurs at the end of January in 2017 and at the end of February in 2018. However, summer 2018 is significantly drier than summer 2017. For the month of August, catchment water balance indicates a decrease of 37 mm between 2017 and 2018 and SG indicates a decrease of 76 mm equivalent water thickness. This strong water deficit observed by both catchment water balance and gravity measurements may result from the rainfall deficit and slightly higher evapotranspiration associated with the 2018

Fig. 3 Top: Comparison between daily SG hydro-gravimetric signal, catchment water balance and MERRA2 local hydrology using an SG admittance scaled on catchment water balance. Bottom: Misfit histograms between SG hydro-gravimetric signal and MERRA2 local (in black) and between SG hydro-gravimetric signal and catchment water balance (in green)



drought. For the period 2014–2018 the mean annual rainfall is 1,194 mm and mean annual evapotranspiration is 418 mm, while in 2018 the mean annual rainfall was 1,079 mm and evapotranspiration was 424 mm.

We compared the SG hydro-gravimetric signal to the local component of the hydrological model MERRA2 (Reichle et al. 2017) computed at EOST (<http://loading.u-strasbg.fr/>). MERRA2 local WSC exhibits less fast WSC than observed by the SG and in addition there is a significant phase shift between both signals. The adjusted admittance we found by scaling the SG signal on MERRA2 local is $0.349 \text{ nm.s}^{-2}.\text{mm Water}^{-1}$ which is outside the range of computed masked admittance values (Fig. 2). This merely point out that MERRA2 local water storage changes are too strong compared to catchment water balance WSC and SG WSC. The mean squared difference between SG (using the admittance scaled on catchment water balance: $0.597 \text{ nm.s}^{-2}.\text{mm Water}^{-1}$) and MERRA2 is 66 mm of water. This relatively poor fit may result from the low spatial resolution (70 km in latitude and longitude) of MERRA2 model as well as the use of satellite data to force it. The need for local measurements of hydrometeorological parameters to conduct hydro-gravimetric studies dedicated to local hydrology was indeed highlighted previously by other studies (e.g. Fores et al. 2017). Our study therefore clearly demonstrates the benefits, especially in a mountainous catchment, of in situ gravity observations with a superconducting gravimeter compared to global hydrological model for the characterization of catchment hydrology.

5 Conclusion

Considering the numerous corrections applied onto the measured gravity signal as well as the hypothesis made to convert the SG hydro-gravimetric signal into WSC (including the simplistic approach used to take into account the building mask effect), it is remarkable to have such a good agreement between WSC derived from SG monitoring and from catchment water balance (mean squared difference of 36 mm of water). It shows that the SG hydro-gravimetric signal is a valuable proxy of WSC in the Strengbach catchment and that nearby catchments may have a similar hydrological behavior. It also demonstrates the benefits of in situ gravity changes observations compared to MERRA2 global hydrological model, especially in mountainous areas with strong topography.

The water cycle is dominated by an annual component but exhibits a strong water deficit due to drought. August 2018 has a water deficit of 37 mm (as inferred from catchment water balance) or 76 mm (as seen by SG) compared to August 2017. Although strong interannual fluctuations of rainfall and catchment WSC have been documented since the beginning of the hydro-meteorological monitoring (1986), such very long and intense drought episodes are unprecedented.

In this study we demonstrated the benefit of superconducting gravimeter observations as a proxy of WSC in a very hydrologically reactive mountainous catchment while most

of the existing hydro-gravimetric studies are focused on the hydrological characterization of relatively flat areas. It therefore expands the area of use of superconducting gravimeters for the hydrological characterization of the critical zone in mountainous contexts. This study is also a step necessary to assess Strengbach forest vulnerability to drought in the context of climate change, and hence to allow the future management of the local forestry.

Acknowledgements We thank J.-P. Boy for providing surface loading computation of MERRA2 hydrological loading and ECMWF atmospheric loading through the EOST loading service (<http://loading.u-strasbg.fr>). iGrav#30 superconducting gravimeter has been funded by EQUIPEX CRITEX (<https://www.critex.fr>). We thank OHGE (<http://ohge.unistra.fr/>) for providing all hydro-meteorological data used in this study. We also thank the doctoral school ED413 from the Strasbourg university as well as ANR HYDROCRIZSTO ANR-15-CE01-0010-02 which provided the funding for this study. We are grateful for the work done by anonymous reviewers which considerably improved this manuscript.

References

- Asner GP et al (2016) Progressive forest canopy water loss during the 2012–2015 California drought. *Proc Natl Acad Sci* 113(2):E249–E255
- Boy JP et al (2002) Reduction of surface gravity data from global atmospheric pressure loading. *Geophys J Int* 149:534–545. <https://doi.org/10.1046/j.1365-246X.2002.01667.x>
- Bréda N et al (2006) Temperate forest trees and stands under severe drought: a review of ecophysiological responses, adaptation processes and long-term consequences. *Ann For Sci* 63:625–644. <https://doi.org/10.1051/forest:2006042>
- Creutzfeldt B et al (2010) Reducing local hydrology from high precision gravity measurements: a lysimeter-based approach. *Geophys J Int* 183:178–187. <https://doi.org/10.1111/j.1365-246X.2010.04742.x>
- Crossley D, Hinderer J (2010) GGP (Global Geodynamics Project): an international network of superconducting gravimeters to study time-variable gravity. In: *Gravity, geoid and earth observation*. Springer, Berlin, pp 627–635
- Déville S et al (2013) On the impact of topography and building mask on time varying gravity due to local hydrology. *Geophys J Int* 192(1):82–93. <https://doi.org/10.1093/gji/ggs007>
- Fores B et al (2017) Assessing the precision of the iGrav superconducting gravimeter for hydrological models and karstic hydrological process identification. *Geophys J Int* 208:ggw396. <https://doi.org/10.1093/gji/ggw396>
- Garnier A et al (1999) A lumped water balance model to evaluate duration and intensity of drought constraints in forest stands. *Ecol Model* 116:269–283. [https://doi.org/10.1016/S0304-3800\(98\)00205-1](https://doi.org/10.1016/S0304-3800(98)00205-1)
- Hector B et al (2013) Gravity effect of water storage changes in a weathered hard-rock aquifer in West Africa: results from joint absolute gravity, hydrological monitoring and geophysical prospection. *Geophys J Int* 194:737–750. <https://doi.org/10.1093/gji/ggt146>
- Hector B et al (2014) Hydro-gravimetry in West-Africa: first results from the Djougou (Benin) superconducting gravimeter. *J Geodyn* 80:34–49. <https://doi.org/10.1016/j.jog.2014.04.003>
- Hinderer J et al (2015) Superconducting gravimetry. In: Schubert G (ed) *Treatise on geophysics*, vol 3, 2nd edn. Elsevier, Oxford, pp 59–115
- Leirião S et al (2009) Calculation of the temporal gravity variation from spatially variable water storage change in soils and aquifers. *J Hydrol* 365:302–309. <https://doi.org/10.1016/j.jhydrol.2008.11.040>
- Llubes M et al (2004) Local hydrology, the Global Geodynamics Project and CHAMP/GRACE perspective: some case studies. *J Geodyn* 38:355–374. <https://doi.org/10.1016/j.jog.2004.07.015>
- Pierret MC et al (2018) The Strengbach catchment: a multidisciplinary environmental sentry for 30 years. *Vadose Zone J* 17(1):180090. <https://doi.org/10.2136/vzj2018.04.0090>
- Reich M et al (2019) Reducing gravity data for the influence of water storage variations beneath observatory buildings. *Geophysics* 84(1):EN15–EN31. <https://doi.org/10.1190/GEO2018-0301.1>
- Reichle et al (2017) Assessment of MERRA-2 land surface hydrology estimates. *J Clim* 30(8):2937–2960. <https://doi.org/10.1175/JCLI-D-16-0720.1>
- Rosat S et al (2018) A two-year analysis of the iOSG-24 superconducting gravimeter at the low noise underground laboratory (LSBB URL) of Rustrel, France: environmental noise estimate. *J Geodyn* 119:1–8. <https://doi.org/10.1016/j.jog.2018.05.009>
- Schuell K (2015) Theoretical basis for earth tide analysis with the new ETERNA34-ANA-V4.0 program. *Bull Inf Marées Terrestres* 149:024–012
- Seneviratne SI et al (2012) Changes in climate extremes and their impacts on the natural physical environment. In: *Managing the risks of extreme events and disasters to advance climate change adaptation, a special report of working groups I and II of the Intergovernmental Panel on Climate Change (IPCC)*. Cambridge University Press, Cambridge, pp 109–230
- Shamir E et al (2016) The use of an orographic precipitation model to assess the precipitation spatial distribution in Lake Kinneret watershed. *Water* 8(12):591. <https://doi.org/10.3390/w8120591>
- Weill S et al (2017) A low-dimensional subsurface model for saturated and unsaturated flow processes: ability to address heterogeneity. *Comput Geosci* 21:301–314. <https://doi.org/10.1007/s10596-017-9613-8>

Open Access This chapter is licensed under the terms of the Creative Commons Attribution 4.0 International License (<http://creativecommons.org/licenses/by/4.0/>), which permits use, sharing, adaptation, distribution and reproduction in any medium or format, as long as you give appropriate credit to the original author(s) and the source, provide a link to the Creative Commons licence and indicate if changes were made.

The images or other third party material in this chapter are included in the chapter's Creative Commons licence, unless indicated otherwise in a credit line to the material. If material is not included in the chapter's Creative Commons licence and your intended use is not permitted by statutory regulation or exceeds the permitted use, you will need to obtain permission directly from the copyright holder.

